Cancer Cells

DOI: 10.1002/anie.201302278

Efficient Isolation and Accurate In Situ Analysis of Circulating Tumor Cells Using Detachable Beads and a High-Pore-Density Filter**

Hun Joo Lee, Jin Ho Oh, Jin Mi Oh, Jong-Myeon Park, Jeong-Gun Lee, Minseok S. Kim, Yeon Jeong Kim, Hyun Ju Kang, Joon Jeong, Seung Il Kim, Soo Suk Lee, Jeong-Woo Choi,* and Nam Huh**

Circulating tumor cells (CTCs) in the bloodstream of cancer patients may indicate the likelihood and severity of metastatic progression. Identification, enumeration, and characterization of CTCs may provide a minimally invasive method for assessing cancer status of patients and prescribing personalized anticancer therapy.[1] However, examination of CTCs requires isolation of these cells from whole blood of patients, which is difficult owing to their low quantity (around one CTC per 10^9 non-cancerous hematopoietic cells in patient blood).[2] Many techniques are used to isolate CTCs, including density gradient centrifugation and dielectrophoresis, but methods using either size-based exclusion or affinity-based enrichment are common.[3] Size-based exclusion assumes that CTCs are larger than most hematopoietic cells and removes all cells smaller than a pre-determined size threshold.[4] Affinity-based enrichment relies on the expression of surface proteins specific to cancer cells and absent in hematopoietic cells. These methods generally use antibody-conjugated magnetic beads and enrich for CTCs by magnetic separation, such as the CellSearch system.[5]

Owing to their heterogeneous nature, it may be practically impossible to isolate CTCs with high isolation efficiency using the aforementioned methods. Some CTCs are reported to be nearly identical in size or even smaller than leukocytes, making them difficult to discriminate by size.[6] As for protein expression, epithelial markers, such as EpCAM (epithelial cell adhesion molecule), are downregulated during epithelial-to-mesenchymal transition (EMT).[7] Furthermore, the type and expression levels of surface proteins may vary greatly depending on cancer histological subtype.[8] Considering these variations, finding the right antibody or combination of antibodies that consistently captures all CTCs may prove to be difficult.

To maximize isolation efficiency, we devised a dual-mode isolation strategy that combines affinity-based enrichment and size-based exclusion.[9] By using microbeads conjugated with CTC-specific antibodies, the size of CTCs can be augmented to enable better discrimination against leukocytes. Subsequent size filtration isolates bead-bound CTCs, allowing the recovery of even smaller-sized CTCs. However, all bead-based capture methods have the inherent limitation of prohibiting accurate image analysis, which is due to optical distortion created by the presence of beads attached to cells. The attached beads not only impede observation of cellular morphology but can actually alter fluorescence signal intensities (Figure 1), demonstrating the incompatibility of in situ quantitative analysis with bead-based capture methods (see the Supporting Information).

Accurate quantification of protein expression can lead to better clinical management, particularly in regards to personalized therapy. The expression levels of predictive biomarkers, such as HER2 and EGFR, are commonly used to match patients with appropriate treatment strategies and predict the effectiveness of anticancer drugs.[10] Therefore, it is important to accurately characterize CTCs, and removal of beads from the surface of CTCs prior to imaging is necessary. Thus, we have developed a new method to detach beads from bead-bound cells: By inserting a photocleavable linker between the bead surface and conjugated antibodies, it is possible to remove the attached beads from cells by light irradiation without affecting cell viability. Herein, we demonstrate a novel approach for isolation and subsequent in situ protein-expression analysis of CTCs using detachable beads termed RIA (reversible bead attachment for cell isolation and analysis).

Scheme 1 illustrates the entire RIA process. Detachable beads conjugated to CTC-specific antibodies bind to CTCs in whole blood of patients. After incubation, the entire sample is filtered through a high-pore-density membrane filter chip, which contains a maximal number of uniform-sized (pore diameter 8 μm) evenly spaced circular pores (distance between pores 5 μm). This step eliminates almost all hematopoietic cells, while CTCs remain on the filter surface. The

[*] H. J. Lee,[+] Dr. J. H. Oh,[+] J. M. Oh, J. M. Park, Dr. J. G. Lee, Dr. M. S. Kim, Dr. Y. J. Kim, Dr. H. J. Kang, Dr. S. S. Lee, Dr. N. Huh
In Vitro Diagnostics Lab, Bio Research Center, Samsung Biomedical Research Institute, Samsung Advanced Institute of Technology
Gyeonggi-do 446-712 (Korea)
E-mail: soosuk@samsung.com
namhuh@samsung.com
H. J. Lee,[+] Prof. J. W. Choi
Interdisciplinary Program of Integrated Biotechnology, Department of Chemical & Biomolecular Engineering
Sogang University, Seoul 121-742, Korea
E-mail: jwchoi@sogang.ac.kr
J. M. Park, Prof. J. Jeong, Prof. S. I. Kim
Department of Chemistry and Center for Bioactive Molecular Hybrids, Department of Surgery, Severance Hospital
Yonsei University, Seoul 120-749 (Korea)
[+] These authors contributed equally to this work.

[**] We would like to thank all of the patients and healthy volunteers who participated in this study thereby enabling this research.
Supporting information for this article is available on the WWW under http://dx.doi.org/10.1002/anie.201302278.

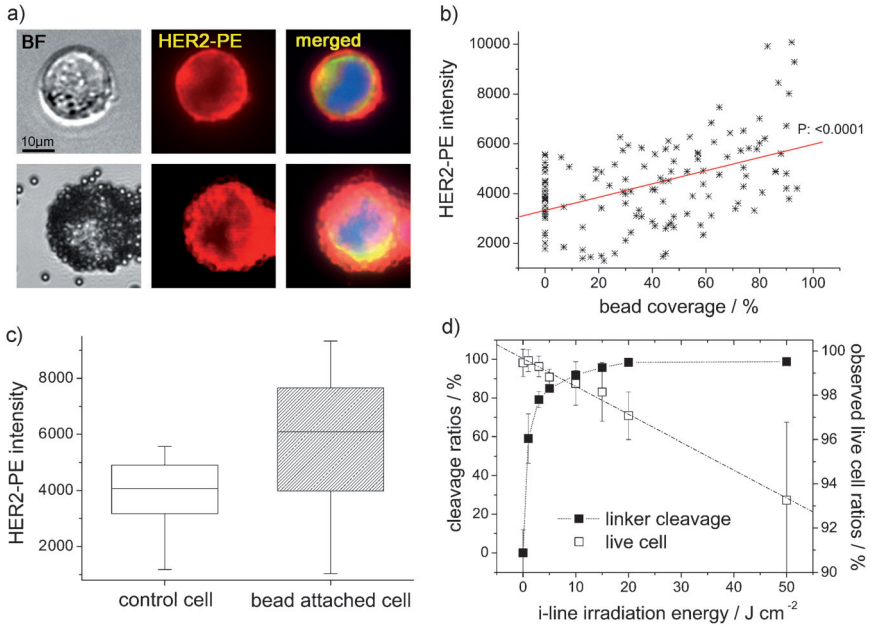

Figure 1. a) Micrographs of control (top) and bead-attached SK-BR-3 cells (bottom). b) Correlation of fluorescence intensities with bead coverage. c) Comparison of fluorescence intensity between control and bead-attached cells. d) Photocleavage efficiency and cell viability after different levels of light exposure.

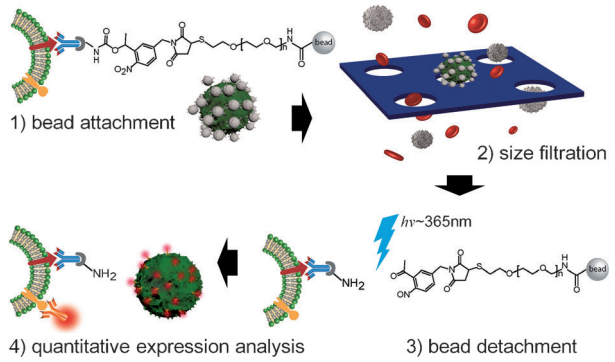

Scheme 1. Illustration of CTC isolation and subsequent in situ protein-expression analysis using RIA. 1) Detachable beads bind to CTCs by conjugated antibodies. 2) Bead-attached cells are filtered through a membrane filter chip. 3) Exposure to i-line irradiation induces photocleavage of the linker between the bead surface and the conjugated antibody, resulting in bead detachment from CTCs. 4) Isolated CTCs are immunostained and their in situ protein-expression levels are assessed.

filter chips are then exposed to i-line light irradiation, which cleaves the linker between the bead and the antibody, causing beads to detach from cells and be removed through the filter. After detachment, filtered cells are immunostained directly at the chip surface and visualized by fluorescence microscopy. Isolated CTCs were enumerated by counting cells that stained positively for nucleus (DAPI) and cytokeratin (CK) but not CD45. Concurrently, in situ protein-expression levels were quantified by co-staining with biomarkers of interest, facilitating cell-by-cell image cytometry. All steps of RIA, from isolation to imaging, can be completed within two hours.

Success of the RIA platform depends on the reversibility of bead attachment. To create detachable beads, we first synthesized a photocleavable linker (BPCL), which contains the photocleavable *o*-nitrobenzyl group.[11] This linker was then placed in between the microbeads (diameter 3 μm) and protein G to improve the orientation of the capture antibody. For our purposes, we created beads conjugated with anti-EpCAM antibodies. The synthesized detachable beads showed high affinity towards tumor cells. Further details on bead synthesis and specificity of the beads to CTCs can be found in the Supporting Information.

Exposure to i-line light causes the decoupling of the *o*-nitrobenzyl moiety in BPCL. To determine the optimal energy input required to cleave BPCL, fluorescein isothiocyanate (FITC)-labeled protein G was conjugated to BPCL-linked beads (the step prior to antibody conjugation) and irradiation was delivered from an LED light source ($\lambda = 365$ nm) at a constant rate. The cleavage ratio increased with more exposure time, and the amount of irradiation energy required to effectively cleave attached beads was calculated to be 20 J cm^{-2} (98.4% cleavage efficiency; delivered in total of 100 s). To ensure that this level of light exposure does not affect cell viability, SK-BR-3 breast cancer cells were exposed to various levels of i-line irradiation, and cell viability was assessed for each level. At input energy of 20 J cm^{-2}, about 97% of cells remained viable, suggesting that negative impact on cell viability is negligible (Figure 1d). All subsequent photocleavage reactions mentioned herein were performed by delivering this amount of energy to the filter chip.

To confirm whether RIA improves the isolation efficiency of CTCs, we used four different human cancer cell lines (MDA-MB-453, SK-BR-3, and BT-474 breast cancer cells and HCT-116 colorectal cancer cells), which are known to have high EpCAM expression.[12] Visual inspection by optical microscopy revealed a significant increase in diameter from the original cell size after bead attachment, enabling enhanced discrimination of tumor cells from leukocytes by size filtration. Blood samples from healthy volunteers spiked with tumor cells were used to compare the isolation efficiency of the RIA platform to conventional size-based exclusion methods, mimicked by filtering cell-spiked blood samples directly without bead incubation. RIA showed significantly better isolation efficiency, especially for smaller cells, such as HCT-116 and MDA-MB-453 cells (Figure 2b). Combining data from these four cell lines, the average isolation efficiency of cells increased from 59.2% using conventional size-based exclusion to 89.1% with RIA. Similarly, cells that do not express EpCAM were also isolated with good efficiency by RIA. MDA-MB-231 breast cancer cells, which do not express

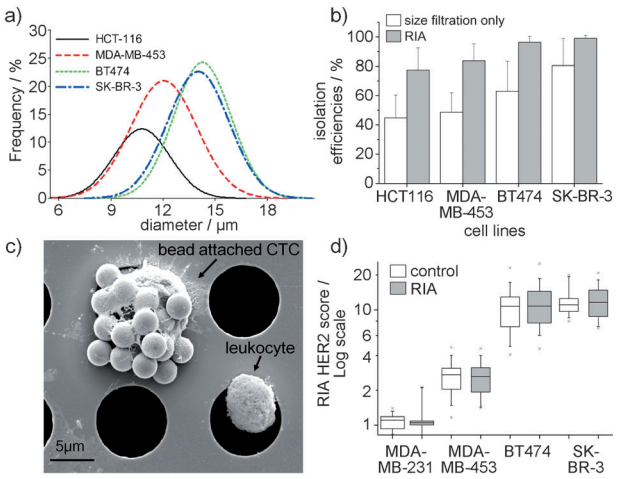

Figure 2. a) Distribution of cell diameters for four different cell types. b) Comparison of isolation efficiencies between conventional size-based exclusion and RIA. c) SEM image of a CTC isolated by the RIA platform. d) Comparison of fluorescence signal intensities in control and RIA-processed cells for cancer cells with different levels of HER2 expression.

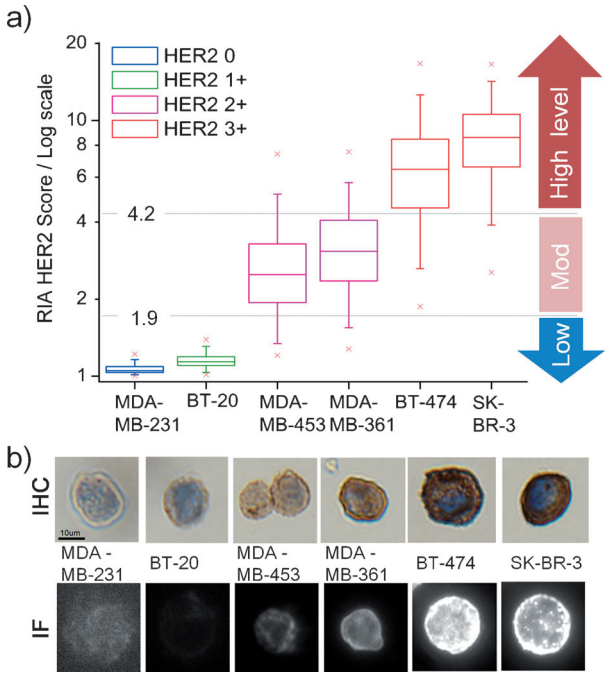

Figure 3. a) HER2 scoring standard generated from various breast cancer cells to categorize HER2 expression of isolated CTCs into three different levels: low, moderate, and high. b) Comparison of HER2 expression by immunofluorescence (IF) using RIA methods and independently-performed immunohistochemistry (IHC).

EpCAM but are generally larger in diameter than leukocytes, were isolated at about 98% with RIA, showing the distinct advantage of RIA over affinity-based enrichment methods. Moreover, the RIA platform with its high-pore-density filter chip demonstrated high purity (< 100 leukocytes/mL), compared to size-based exclusion method using a track-etched membrane. Overall, the isolation efficiency and purity of the RIA platform were on par or better than other well-known CTC isolation methods (see the Supporting Information).

To verify that bead detachment does not affect in situ expression analysis, HER2 was used to compare tumor cells isolated by the RIA platform to a control group (no bead incubation). Expression levels were calculated by taking the average fluorescence intensity within the region of interest (ROI) for a single cell and dividing this value by the average intensity in all non-ROI regions to yield a numerical value, termed RIA HER2 score. As shown in Figure 2d, RIA HER2 scores of cells isolated by RIA were nearly identical to cells in the control group for all cell lines tested. These results confirm that post-isolation cleavage of beads does not affect image-based quantification.

To quantitatively analyze isolated CTCs, we created a scoring standard for cellular HER2 expression using six different breast cancer cell lines with well-known HER2 expression levels (Figure 3a).[13] RIA HER2 scores for each cell type was first measured, and based on this distribution, we determined appropriate thresholds to categorize individual cellular HER2 expression into three groups (low, moderate, or high). The validity of using RIA HER2 scores to classify HER2 expression levels was confirmed by immunohistochemistry (Figure 3b) and western blotting.

We then applied the RIA platform along with its HER2 scoring standard to clinical samples. Peripheral blood samples were obtained from 12 metastatic breast cancer patients. CTCs were identified in all samples, with numbers ranging from 1 to 31 CTCs per mL (Figure 4a). In half of the patients, we found CTC clusters, herein defined as complexes with two or more adjoined CTCs (Figure 4b). Using RIA HER2 scoring standard, HER2 expression of isolated CTCs were evaluated and compared to the corresponding HER2 status of the primary breast cancer tissues. 67% overall concordance was observed between HER2 scores of CTCs and primary tissues. For patients with low levels of HER2 expression in primary tissues, 5 of 6 samples also exhibited low HER2 expression in isolated CTCs. HER2 expression in isolated CTCs was quite heterogeneous, with 10 of 12 samples containing CTCs with different HER2 expression levels. These results suggest that CTCs are heterogeneous and may exhibit different characteristics from their originating primary tissues. Interestingly however, in all patient samples with identified CTC clusters, cells comprising a single cluster had identical HER2 expression levels, suggesting that cells forming the cluster may originate from a single source. Further studies are necessary to better understand the clinical significance of our findings.

In conclusion, we have demonstrated that the RIA platform is capable of not only isolating CTCs from metastatic cancer patients but also characterizing them based on their in situ protein-expression levels. RIA includes a novel method for isolating CTCs by combining affinity-based reversible bead attachment and size-based exclusion assay, especially improving the isolation efficiency of small-sized CTCs. At the same time, protein-expression levels of isolated cells were accurately assessed, without optical distortion, using detachable beads. Thus, RIA can be extended to visualize and quantify in situ expression of CTCs for a wide

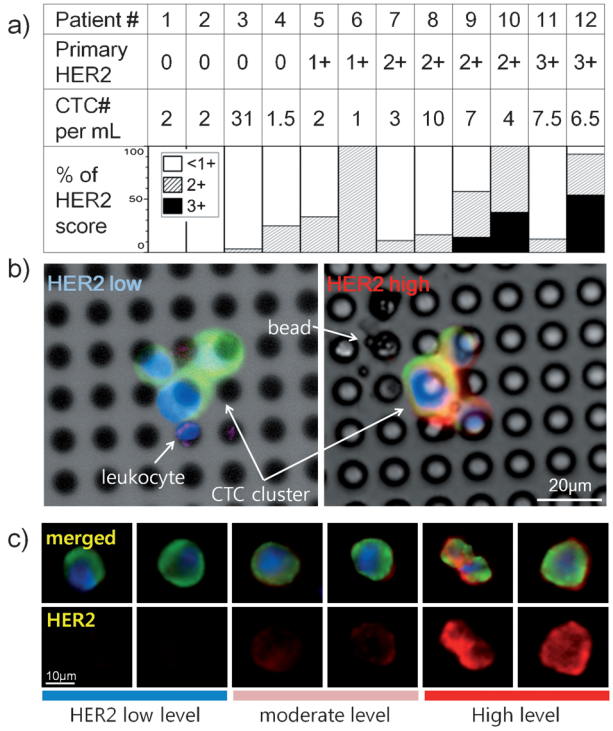

Figure 4. a) Enumeration and HER2 expression analysis of CTCs isolated from metastatic breast cancer patients using the RIA platform, along with HER2 expression levels in primary tissues. b) Visualization of CTC clusters on the filter chip surface. (DAPI: blue; CK: green; HER2: red; CD45: pink) c) Different levels of HER2 expression in CTCs isolated from patients.

range of biomarkers. These could be applicable for better understanding of cancer progression, metastasis monitoring, appropriate selection (or combination) of anticancer drugs, and other cancer therapy techniques to improve clinical outcomes. With further development, we expect that the RIA platform can play a critical role in the early diagnosis of cancer, personalized anticancer therapy, and regular monitoring of cancer recurrence.

Received: March 18, 2013
Revised: May 20, 2013
Published online: July 3, 2013

Keywords: cancer · cell capture · circulating tumor cells · in situ analysis · photolysis

[1] a) M. Cristofanilli et al., *N. Engl. J. Med.* **2004**, *351*, 781 – 791 (see the Supporting Information (SI) for authors); b) P. Paterlini-Brechot, N. L. Benali, *Cancer Lett.* **2007**, *253*, 180 – 204; c) K. Pantel, S. Riethdorf, *Nat. Rev. Clin. Oncol.* **2009**, *6*, 190 – 191.
[2] a) S. Nagrath et al., *Nature* **2007**, *450*, 1235 – 1239 (see the SI); b) K. Pantel, C. Alix-Panabieres, *Trends Mol. Med.* **2010**, *16*, 398 – 406.
[3] a) H. W. Hou et al., *Sci. Rep.* **2013**, *3*, 1259 (see the SI); b) S. Wang et al., *Angew. Chem.* **2011**, *123*, 3140 – 3144; *Angew. Chem. Int. Ed.* **2011**, *50*, 3084 – 3088; c) S. Balasubramanian et al., *Angew. Chem.* **2011**, *123*, 4247 – 4250; *Angew. Chem. Int. Ed.* **2011**, *50*, 4161 – 4164; d) W. He, S. A. Kularatne, K. R. Kalli, F. G. Prendergast, R. J. Amato, G. G. Klee, L. C. Hartmann, P. S. Low, *Int. J. Cancer* **2008**, *123*, 1968 – 1973; e) V. Gupta, I. Jafferji, M. Garza, V. O. Melnikova, D. K. Hasegawa, *Biomicrofluidics* **2012**, *6*, 024133.
[4] a) G. Vona et al., *Am. J. Pathol.* **2000**, *156*, 57 – 63 (see the SI); b) M. C. Liu, Y. C. Tai, *Biomed. Microdevices* **2011**, *13*, 191 – 201; c) H. Mohamed, M. Murray, J. N. Turner, M. Caggana, *J. Chromatogr. A* **2009**, *1216*, 8289 – 8295.
[5] a) E. A. Punnoose et al., *PLoS One* **2010**, *5*, e12517 (see the SI); b) A. H. Talasaz et al., *Proc. Natl. Acad. Sci. USA* **2009**, *106*, 3970 – 3975; c) H. Engel, C. Kleespies, J. Friedrich, M. Breidenbach, A. Kallenborn, T. Schondorf, H. Kolhagen, P. Mallmann, *Br. J. Cancer* **1999**, *81*, 1165 – 1173.
[6] a) M. Alunni-Fabbroni, M. T. Sandri, *Methods* **2010**, *50*, 289 – 297; b) D. Marrinucci et al., *Phys. Biol.* **2012**, *9*, 016003 (see the SI).
[7] T. M. Gorges, I. Tinhofer, M. Drosch, L. Rose, T. M. Zollner, T. Krahn, O. von Ahsen, *BMC Cancer* **2012**, *12*, 178.
[8] a) A. Goldhirsch et al., *Breast. Cancer Res.* **2011**, *13*, R87 (see the SI).
[9] a) M. S. Kim et al., *Lab Chip* **2012**, *12*, 2874 – 2880 (see the SI).
[10] a) C. L. Vogel et al., *J. Clin. Oncol.* **2002**, *20*, 719 – 726 (see the SI); b) L. V. Sequist, D. W. Bell, T. J. Lynch, D. A. Haber, *J. Clin. Oncol.* **2007**, *25*, 587 – 595.
[11] a) D. Saran, D. H. Burke, *Bioconjugate Chem.* **2007**, *18*, 275 – 279; b) J. Szychowski, A. Mahdavi, J. J. Hodas, J. D. Bagert, J. T. Ngo, P. Landgraf, D. C. Dieterich, E. M. Schuman, D. A. Tirrell, *J. Am. Chem. Soc.* **2010**, *132*, 18351 – 18360; c) H. Y. Song, M. H. Ngai, Z. Y. Song, P. A. MacAry, J. Hobley, M. J. Lear, *Org. Biomol. Chem.* **2009**, *7*, 3400 – 3406; d) X. Tang, I. J. Dmochowski, *Nat. Protoc.* **2007**, *1*, 3041 – 3048.
[12] a) N. Prang et al., *Br. J. Cancer* **2005**, *92*, 342 – 349 (see the SI); b) I. L. Botchkina et al., *Cancer Genomics Proteomics* **2009**, *6*, 19 – 29.
[13] a) M. Ignatiadis et al., *PLoS One* **2011**, *6*, e15624 (see the SI); b) S. Riethdorf et al., *Clin. Cancer Res.* **2010**, *16*, 2634 – 2645.

